CHEMISTRY OF MATERIALS
Article

Chem. Mater. **2010,** *22,* 5345–5349 5345
DOI:10.1021/cm101657z

Selective Detection of Cs^+ in Water Solutions via One-Step Formation of a New Type of Struvite-Like Phosphate

Stanislav Ferdov*,† and Zhi Lin*,‡

†*Department of Physics, University of Minho, 4800-058 Guimares, Portugal, and* ‡*Departments of Chemistry, CICECO, University of Aveiro, 3810-193 Aveiro, Portugal*

Received June 14, 2010. Revised Manuscript Received August 11, 2010

We report an inorganic, highly selective structural sensor for cesium ions that effectively works at room temperature in water solutions with different competing alkaline elements. The process of sensing realizes via selective transformation of $Na_3MnH(P_{0.9}O_4)_2$ to a new type of struvite-like cesium-containing solid $CsMn(PO_4)\cdot 6H_2O$. The inclusion of the cesium in the structure is stable and no reverse exchange is possible.

Introduction

Radioactive cesium contamination of water is of serious social and environmental concern because it is a significant fraction of the radioactivity of the liquid waste from the reprocessing of nuclear fuel.[1] For instance, it is estimated 65 million gallons of waste stored in stainless steel tanks in the Hanford reservation in Washington State which was produced as a result of the reprocessing of irradiated uranium fuel to recover ^{239}Pu for weapons manufacture.[2] A number of these tanks have leaked, resulting in contamination of the groundwater with radionuclides such as ^{137}Cs and ^{90}Sr.[3] Similar groundwater contamination problems also occur at other nuclear sites such as the Idaho National Engineering and Environmental Laboratory (INEEL).[4] Once leaked, cesium-137 transfers through different aquatic trophic levels involving the adsorption and absorption by aquatic plants, ingestion by fish, and subsequent accumulation in piscivorous birds or mammals at the top of the food chain.[5,6] Consequently, there is considerable interest to develop cesium selective sensors that can be utilized to perform in situ detection of cesium ions in different aquas solutions. In this respect, a cheap, unabigous, and harmless detection of cesium ions is still a challenge. To date, the main known sensors of cesium ions are based on atomic absorption spectroscopy,[7] radioanalysis,[8,9] and ion-selective electrodes (ISEs)[10−12] which have a good sensitivity but require expensive instruments and/or controlled experimental conditions. More recently, different types of fluorescent molecular sensors are receiving an increasing attention because of their excellent selectivity to cesium ions,[13−19] but their applications are limited by the requirements for certain solubility and the right choice of the sensing ionophore for given conditions.[14] Here we report a new type of sensor, which is inorganic and it detects cesium ions via structure transformation of $Na_3MnH(P_{0.9}O_4)_2$[20] to $CsMn(PO_4)\cdot 6H_2O$ at room temperature in presence of other competing alkaline ions. The detection of cesium is not spectroscopic and it is based on a collection of an ordinary powder X-ray diffraction pattern.

Experimental Section

Synthesis. The synthesis of $NaMnH(P_{0.9}O_4)_2$ was performed according to our previously reported recipe. Namely, a solution of 0.47 g of NaH_2PO_4 (Aldrich) in 8.67 g of distilled water was

*Corresponding author. E-mail: sferdov@fisica.uminho.pt; zlin@ua.pt.

(1) Northrup, C. J.; Jardine, L. J.; Steindler, M. J. *IAEA-SM-261/31*; International Atomic Energy Agency: Vienna, 1983; p 461.
(2) Zorpette, G. Sci. Am. May **1996**, 88.
(3) Keller, J. F.; Stewart, T. L. *Proceedings of the First Hanford Separation Science Workshop*; Richland WA, July 23−25, 1991; Pacific Northwest Laboratory: Richland, WA, 1993; p I.35.
(4) Garn, T. G.; Brewer, K. N.; Tillotson, R. D.; Todd, T. A. *Demonstration of Various Ion Exchange Sorbents for the Removal of Cesium and Strontium from TAN Groundwater*; Report INEEL/EXT-97-00825; Idaho National Engineering and Environmental Laboratory: Idaho Falls, ID, August 1997.
(5) Davis, J. J.; Foster, R. F. *Ecology* **1958**, *39*, 530.
(6) Shure, D. J.; Gottschalk, M. R. Cesium-137 dynamics within a reactor effluent stream in South Carolina. In *Radioecology and Energy Resources*; Cushing, C. E., Ed.; Dowden, Hutchinson and Ross, Inc.: Stroudsburg, PA, 1976; pp 234−241.
(7) Vanhoe, H.; Vandecasteele, C.; Versieck, J.; Dams, R. *Anal. Chem.* **1989**, *61*, 1851.
(8) Theimer, K. H.; Krivan, V. *Anal. Chem.* **1990**, *62*, 2722.
(9) Van-Renterghem, D.; Cornelis, R.; Vanholder, R. *Anal. Chim. Acta* **1992**, *257*, 1.
(10) Saleh, M. B.; Hassan, S. S. M.; Abdel Gaber, A. A.; Abdel Kream, N. A. *Anal. Lett.* **2003**, *36*, 2367.
(11) Arida, H. A. M.; Aglan, R. F.; El-Reefy, S. A. *Anal. Lett.* **2004**, *37*, 21.
(12) Radu, A.; Peper, S.; Gonczy, C.; Runde, W.; Diamond, D. *Electroanalysis* **2006**, *18*, 1379.
(13) Ji, H.-F.; Brown, G. M.; Dabestani, R. *Chem. Commun.* **1999**, 609.
(14) Souchon, V.; Leray, I.; Valeur, B. *Chem. Commun.* **2006**, 4224.
(15) Casnati, A.; Pochini, A.; Ungaro, R.; Ugozzoli, F.; Arnaud, F.; Fanni, S.; Schwing, M.-J.; Egberink, R. J. M.; de Jong, F.; Reinhoudt, D. N. *J. Am. Chem. Soc.* **1995**, *117*, 2767.
(16) Wintergerst, M. P.; Levitskaia, T. G.; Moyer, B. A.; Sessler, J. L.; Delmau, L. H. *J. Am. Chem. Soc.* **2008**, *130*, 4129.
(17) Webber, P. R. A.; Beer, P. D.; Chen, G. Z.; Felix, V.; Drew, M. G. B. *J. Am. Chem. Soc.* **2003**, *125*, 5774.
(18) Arnaud-Neu, F.; Asfari, Z.; Souley, B.; Vicens, J. *New J. Chem.* **1996**, *20*, 453.
(19) Lamare, V.; Dozol, J. F.; Fuangswasdi, S.; Arnaud-Neu, F.; Thuery, P.; Nierlich, M.; Asfari, Z.; Vicens, J. *J. Chem. Soc., Perkin Trans.* **1999**, *2*, 271.
(20) Ferdov, S.; Lopes, A. M. L.; Lin, Z.; Ferreira, R. A. S. *Chem. Mater.* **2007**, *19*, 6025.

Published on Web 08/25/2010

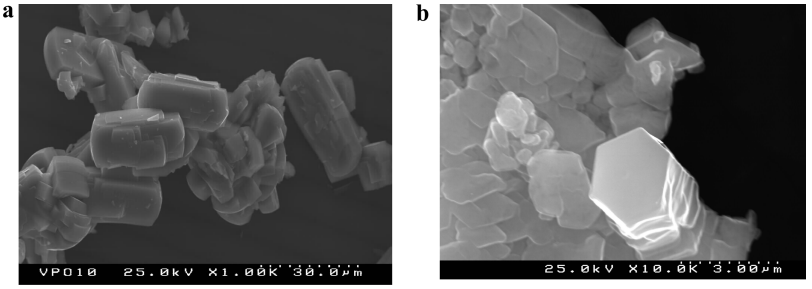

Figure 1. SEM images of (a) prismatic $Na_3MnH(P_{0.9}O_4)_2$ particles and their transformation to (b) hexagonal $CsMn(PO_4)\cdot 6H_2O$ ones after immersing in cesium-containing solution.

mixed with 13.28 g of MPMD (Du Pont). Then, 0.05 g of $MnSO_4\cdot H_2O$ (Aldrich) dissolved in 6.58 g of distilled water was added to the above solution. The resulting mixture was homogenized for 40 min and then transferred into a Teflon-lined autoclave (45 mL). The crystallization was performed under static conditions at 150 °C for 6 days. After fast cooling with flowing water, the run product was filtered with distilled water and dried at 40 °C for 1 day. The success of the synthesis was verified by powder X-ray diffraction.

Behavior in Alkaline Solutions. Different concentration of aqueous solutions of LiCl, KCl, RbCl and CsCl (Aldrich, purity of more than 99.5%.), were prepared. Then, 100 mg of $Na_3MnH(P_{0.9}O_4)_2$ was immersed in the salt solution for two days at room temperature, without agitation. The solid was separated from the solution by filtration with filter paper, washed with distilled water, and dried at room temperature.

Powder X-ray Diffraction (XRD) Data Collection. Powder XRD data were collected on a Philips X'pert MPD diffractometer (Cu Kα X radiation) using a fixed divergence slit of 0.25°, and a flat-plate sample holder, in a Bragg−Brentano parafocusing optics configuration. The diffraction intensity was collected by the step scan method. For phase identification it was used a step of 0.04, time per step 1s, and range 5−50°. The structural solution and Rietveld refinement were performed from pattern collected in the 2θ range between 13 and 115°, step 0.04° and time 10 s per step.

Further Characterization Methods. Fourier transform infrared (FTIR) spectrum of powdered sample suspended in KBr pallets was acquired between 400 and 4000 cm^{-1} using a Mattson 7000 spectrometer, with resolution 2 cm^{-1}. The thermogravimetry (TG) curve was collected with a Shimadzu TG-50 analyzer. The sample was heated in air at a rate of 5 °C min^{-1}. The scanning electron microscopy images and chemical analysis (energy-dispersive spectrometry, EDS) were carried out using a scanning electron microscope, Hitachi S-4100, equipped with a Römteck EDS system.

Results and discussion

Ab initio Structural Determination. After $Na_3MnH(P_{0.9}O_4)_2$ was immersed in solution containing cesium ions, the initial prismatic particles were transformed to hexagonal-like plates (the duration of the reaction was 72 h) which together with the collected XRD different pattern suggested a new structure (Figure 1). The XRD peak positions and relative intensities were accurately determined by the software package TOPAS-3.[21] The extracted information was included in the indexing program TREOR90,[22] which indicated a hexagonal unit cell. The same cell was confirmed by DICVOL91.[23] The choice of the space group in the estimated hexagonal system was made by examination of the systematic absences[24] which pointed out five possible space groups: $P6_3mc$, $P\bar{6}2c$, $P6_3/mmc$, $P3c1$ and $P\bar{3}1c$. The structure was successfully solved in $P6_3mc$. The ab initio crystal structure determination was carried out with the EXPO package.[25] First, the structure factor amplitudes were extracted by the Le Bail method.[26] Using this information the structure was solved by combining direct methods and difference Fourier synthesis at different angular range. The obtained structural model was validated using the method of Rietveld. The refinement was performed by FullProf[27] software package in the range 13−100° 2θ for 332 independent reflections involving the parameters shown in Table S1 in the Supporting Information. The final Rietveld plot is shown in Figure 2, and the refined atomic coordinates are given in Table S2 in the Supporting Information. Within experimental error, the EDS

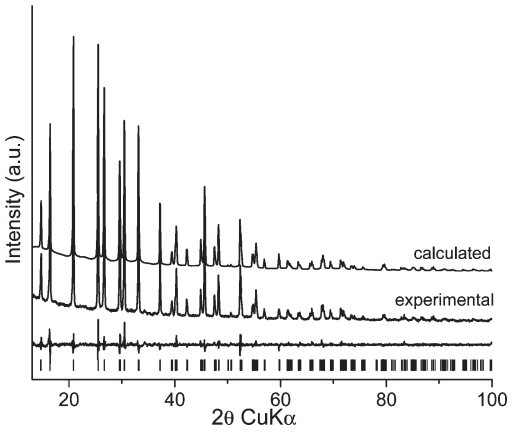

Figure 2. Experimental and simulated powder XRD patterns of $CsMn(PO_4)\cdot 6H_2O$.

(21) *TOPAS V3.0: General Profile and Structure Analysis Software for Powder Diffraction Data*; Bruker AXS: Karlsruhe, Germany.
(22) Werner, P. E.; Eriksson, L.; Westdahl, M. *J. Appl. Crystallogr.* **1985**, *18*, 367.
(23) Boultif, A.; Louër, D. *J. Appl. Crystallogr.* **1991**, *24*, 987.
(24) Laugier, J.; Bochu, B. *CHECKCELL*; Laboratoire des Matériaux et du Génie Physique, École Nationale Supérieure de Physique de Grenoble (INPG) Domaine Universitaire BP 46: 38402 Saint Martin d'Hères, France, 2000.
(25) Altamore, M. C.; Burla, G.; Cascarano, C.; Giacovazzo, A.; Guagliardi, A. G. G.; Moliterni, Polidori, G. *J. Appl. Crystallogr.* **1995**, *28*, 842.
(26) Le Bail, A.; Duroy, H.; Fourquet, J. L. *Mater. Res. Bull.* **1988**, *23*, 447.
(27) Roisnel, T.; Rodriguez-Carvajal, J. WinPLOTR June 2005 A Windows Tool for Powder Diffraction Pattern Analysis. In Materials Science Forum. In *Proceedings of the Seventh European Powder Diffraction Conference* (*EPDIC 7*); Barcelona, May 20−23, 2000; Delhez, R., Mittenmeijer, E. J., Eds.; Trans Tech: Enfield, NH, 2000; pp 118−123.

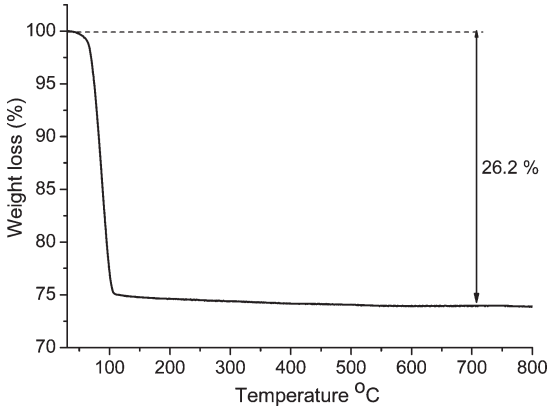

Figure 3. TG curve of $CsMn(PO_4)\cdot 6H_2O$.

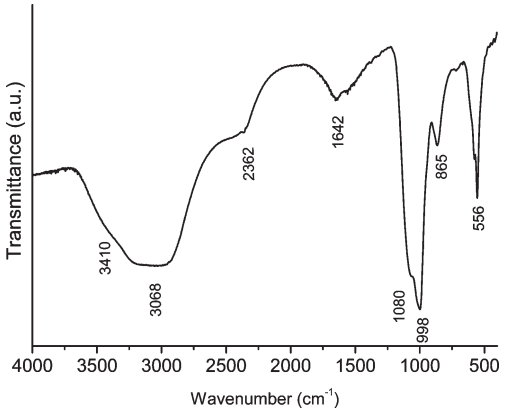

Figure 4. FTIR spectrum of $CsMn(PO_4)\cdot 6H_2O$.

chemical analysis supports the Cs/Mn/P (1:0.7:0.9) ratio obtained by powder XRD (1:1:1). Despite the relative simplicity of the crystal structure, no identical manganese phosphate has been found in the literature and Inorganic Crystal Structure Database (ICDD). However, we came across a isotypic magnesium compound with struvite-like structure $CsMg(OH_2)_6(PO_4)$, where the octahedral Mn site is occupied by Mg, which is coordinated by six water molecules.[28−30]

TG and FTIR. The TG curve of $CsMn(PO_4)\cdot 6H_2O$ is composed of only one step (Figure 3) showing a total mass loss of 26.2%. Considering that no isolated water molecules were detected from the Rietveld refinement it was supposed that the estimated weight loss should be due to release of water molecules participating in the octahedral coordination of Mn site, similar to the water coordination of Mg in the isotypic $CsMg(OH_2)_6(PO_4)$.[29−31] This suggestion is supported by the fact that the total weight loss is in fair agreement with the calculated 6 molecules of water. The dehydration almost completes at about 110 °C and after this temperature the TG curve does not indicate any significant weight loss. The FTIR transmittance spectrum (Figure 4) of $CsMn(PO_4)\cdot 6H_2O$ also shows abundance of hydrous species. A strong broad shoulder peak with two maxima at 3410

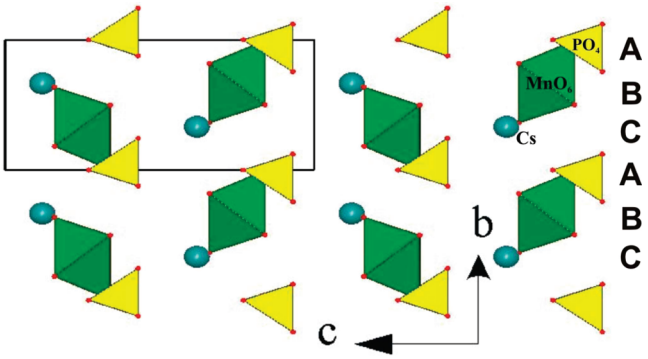

Figure 5. Crystal structure of $CsMn(PO_4)\cdot 6H_2O$ viewed along the *a* axis. The water molecules (not shown) are supposed to coordinate the MnO_6 octahedra.

and 3068 cm^{-1} can be assigned to water $\nu_1-\nu_3$ symmetric and asymmetric stretching modes, respectively.[32] The weak peak at 2362 cm^{-1} is typical for water-phosphate hydrogen bonding (water ν_2, H−O−H) and the broad band at 1640 cm^{-1} is well-known for H−O−H bond bending and it points out the presence of water molecules[33] The shoulder peak at 1080 cm^{-1} and the strong sharp band at 998 cm^{-1} can be assigned to the ν_3 asymmetric P−O stretching and ν_1 P−O symmetric stretching of the PO_4 tetrahedra, respectively. In fact, the splitting of the ν_3 asymmetric stretch absorption band that occurs near 1000 cm^{-1} is a quantitative measure of deviation of the PO_4 group from ideal tetrahedral symmetry, which is also confirmed by the X-ray diffraction analyses. The strong sharp peak at 556 cm^{-1} could be due to ν_4 P−O bending vibrations.[32]

Structural Description. The structure of $CsMn(PO_4)\cdot 6H_2O$ can be viewed as stacking of three types of layers along the *a* axis (Figure 5) in a sequence ABCABC..., where layer A is composed of PO_4^{3-} tetrahedra, layer B of distorted $Mn(H_2O)_6^{2+}$ octahedra, and layer C of charge-compensating cesium cations which form highly irregular cuboctahedra (see Table S3 in the Supporting Information). The structure of $CsMn(PO_4)\cdot 6H_2O$ has features similar to those for the hexagonal struvite analog[29,30] and it represents the first struvite-type phosphate compound that contains Mn as divalent cation. The P−O bond distances range from 1.520(5) to 1.564(9) Å, which is in a fair agreement with the corresponding bond valence sum for P (see Table S3 in the Supporting Information) and previously reported P−O bonds.[29,30] Mn-Ow bond lengths range from 2.079(5) to 2.338(8) Å. Hence the bond valence sums[34] for P and Mn show no anomalities and are in the expected ranges and close to the theoretical values of 5 (P) and 2 (Mn), respectively. However, the corresponding bond valence parameters calculated for Cs^+ (0.59 valence units) indicate a considerable undersaturation with respect to the expected bond valence of 1. This effect may be due to a disorder over the big cesium cation although the resolution of the current

(28) Weil, M. *Acta Crystallogr., Sect. E* **2008**, *64*, i50.
(29) Weil, M. *Cryst. Res. Technol.* **2008**, *43*, 1286.
(30) Massa, W.; Yakubovich, O. V.; Dimitrova, O. V. *Acta Crystallogr., Sect. C* **2003**, *59*, i83.
(31) Ferraris, G.; Fuess, H.; Joswig, W. *Acta Crystallogr., Sect. B* **1986**, *42*, 253.
(32) Banks, E.; Chianell, R.; Korenstein, R. *Inorg. Chem.* **1975**, *14*, 1634.
(33) Beran, A.; Voll, D.; Schneider, H. In *Spectroscopic Methods in Mineralogy*; Beran, A., Libowitzky, E., Eds.; Eötvös University Press: Budapest, 2004; pp 189−226.
(34) Lufaso, M. W.; Woodward, P. M. *Acta Crystallogr., Sect. B* **2001**, *57*, 725.

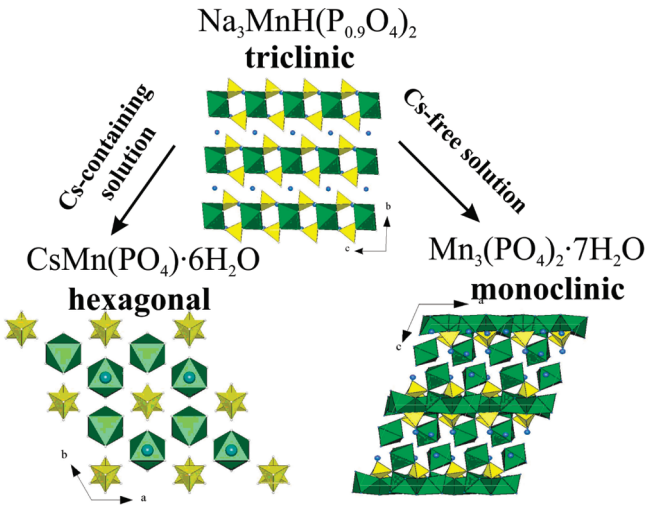

Figure 6. Schematic presentation of the way of detection of cesium ions via selective phase transformation of $Na_3MnH(P_{0.9}O_4)_2$ to $Mn_3(PO_4)_2\cdot 7H_2O$ or $CsMn(PO_4)\cdot 6H_2O$.

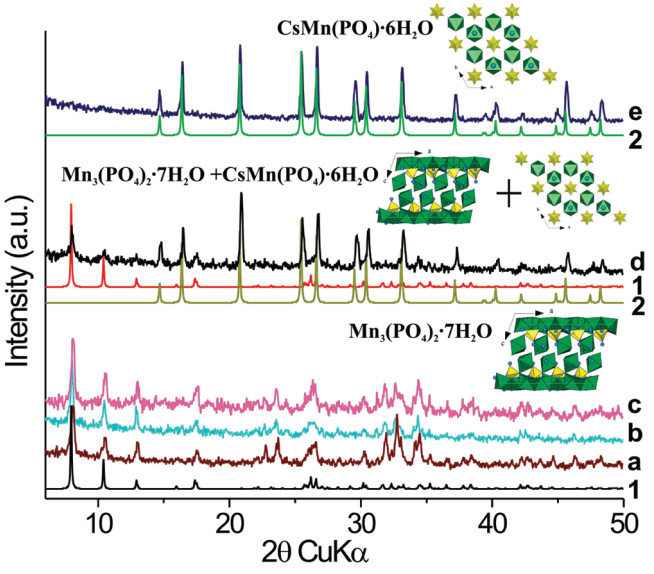

Figure 7. Powder XRD patterns showing the phases obtained after immersing $Na_3MnH(P_{0.9}O_4)_2$ in (a) pure water, (b) 0.001, (c) 0.003, (d) 0.01, and (e) 1 M solutions of CsCl. The obtained XRD patterns are compared with the calculated ones of the mineral switzerite $Mn_3(PO_4)_2\cdot 7H_2O$ (1) and $CsMn(PO_4)\cdot 6H_2O$ (2).

data set cannot clearly indicate this suggestion. The estimated behavior is also reflected by the large average Cs−O distance of 3.92 Å. The undersaturation of the bond valence requirement for cesium cation might also explain its cooperatively large displacement parameters (see Table S2 in the Supporting Information).

Sensing Properties. $Na_3MnH(P_{0.9}O_4)_2$ was synthesized and structurally and magnetically characterized by us[20] and it represents a layered antiferromagnetic material containing structural defects. Immersing $Na_3MnH(P_{0.9}O_4)_2$ in pure water or alkaline water solutions results in specific structural transformations that are sensitive to the presence or absence of cesium ions (Figure 6). In pure water, $Na_3MnH(P_{0.9}O_4)_2$

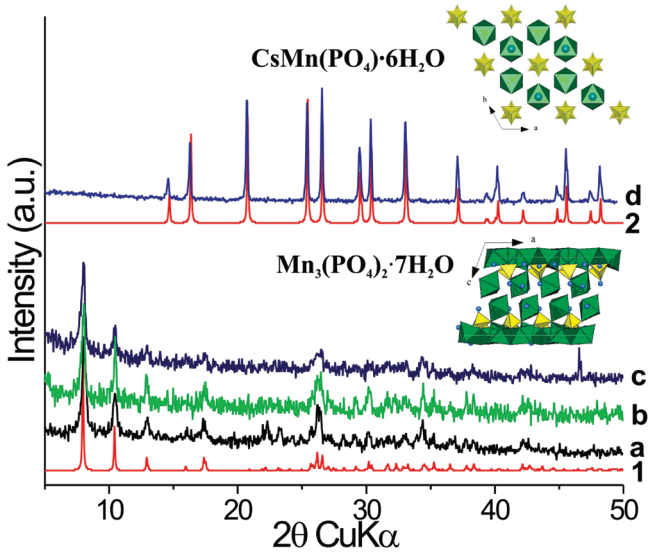

Figure 8. Powder XRD patterns showing the phases obtained after immersing $Na_3MnH(P_{0.9}O_4)_2$ in 1 M solutions of (a) LiCl, (b) KCl, (c) RbCl and (d) a mixture of 1 M solutions of LiCl, NaCl, KCl, RbCl, and CsCl. The obtained XRD patterns are compared with the calculated ones of the mineral switzerite $Mn_3(PO_4)_2\cdot 7H_2O$ (1) and $CsMn(PO_4)\cdot 6H_2O$ (2).

transforms to a phase whose majority of diffraction peaks coincide with the ones of the mineral switzerite ($Mn_3(PO_4)_2\cdot 7H_2O$)[35] (Figure 7a,1). The same effect was observed when $Na_3MnH(P_{0.9}O_4)_2$ is immersed in 1 M (all calculated molarities of the used alkaline solutions are based on 10 mL of water that contains 0.1 g of sample[20]) solutions of KCl, LiCl or RbCl for 72 h at room temperature. This indicates that $Na_3MnH(P_{0.9}O_4)_2$ is indifferent to the used alkaline elements. However, adding small amounts of cesium ions (in form of CsCl) results in transformation of $Na_3MnH(P_{0.9}O_4)_2$ to a new type of struvite-like material $CsMn(PO_4)\cdot 6H_2O$ whose structure was solved ab initio and subsequently refined. The estimated threshold of sensitivity of this transformation is 0.01 M of cesium ions (Figure 7b−d,2). Thus, when the concentration of cesium is 0.01 M the result is a mixture of $Mn_3(PO_4)_2\cdot 7H_2O$ and $CsMn(PO_4)\cdot 6H_2O$ (Figure 7d). Increasing the cesium concentration to 0.1 M the only phase that crystallizes is $CsMn(PO_4)\cdot 6H_2O$ and the same effect is observed in concentration up to 1 M (Figure 7e). In concentrations of cesium ions less than 0.01 M it is formed only $Mn_3(PO_4)_2\cdot 7H_2O$ (Figure 7b). When other alkaline ions (Li, K, Rb) with concentration of 1 M are used instead of cesium, the run product is indifferent to them and $Na_3MnH(P_{0.9}O_4)_2$ always transforms to $Mn_3(PO_4)_2\cdot 7H_2O$ (Figure 8a−c,1). Within these experiments, the most noteworthy finding is that cesium can be also detected in multiple alkaline solutions. Thus, in mixture of 1 M solutions of NaCl, KCl, LiCl, and RbCl it can be detected 1 M concentration of cesium ions as $Na_3MnH(P_{0.9}O_4)_2$ transforms to $CsMn(PO_4)\cdot 6H_2O$ (Figure 8d, 2). When the concentration of cesium is lower than 1 M (0.1 M) then $Na_3MnH(P_{0.9}O_4)_2$ stays unchanged with the time (see Figure S1 in the Supporting Information). This indicates that $Na_3MnH(P_{0.9}O_4)_2$ can be stabilized in super concentrated salt alkaline solutions where the cesium ions do not exceed certain concentration. The pH range

(35) Zanazzi, P. F.; Leavens, P. B.; White, J. S. *Am. Mineral.* **1986**, *71*, 1224.

where $Na_3MnH(P_{0.9}O_4)_2$ was estimated to be a proper material for detection of cesium ions is between 6 and 10 as above these values the material is not stable and within 24 h transforms to unknown phase. Immersing $CsMn(PO_4)\cdot 6H_2O$ in 1 M solution of NaCl for 72 h at room temperature shows that the incorporation of cesium in the structure of $CsMn(PO_4)\cdot 6H_2O$ is stable (see Figure S2 in the Supporting Information) and it cannot be released back to the solution, which also makes $Na_3MnH(P_{0.9}O_4)_2$ a proper material for purification of cesium contaminations in water.

A possible reason for the observed behavior of $Na_3MnH(P_{0.9}O_4)_2$ can originate from the presence of defects in the phosphor sites[20] that makes the material metastable in water or alkaline water solutions of certain concentration. This can cause decomposition and subsequent recrystallization which is directed by the presence or absence of cesium ions. Possibly because of their bigger size and higher electropositive character, cesium ions have an advantage over the competing Li^+, $Na,^+$ K^+, and Rb^+ ions, and in the presented conditions it is the only alkaline cation that can provoke the formation of hexagonal struvite-like material, which is an undoubtful indicator for the presence of cesium ions in the solution. These properties define $Na_3MnH(P_{0.9}O_4)_2$ as a new type of sensor with high affinity to cesium ions that can work in solutions containing other competing cations.

Conclusions

The most noteworthy finding to emerge from this study is that $Na_3MnH(P_{0.9}O_4)_2$ is a new inorganic sensor with selectivity to cesium ions that can work at room temperature in different types and concentrations of competing alkaline cations in water solutions. The detection of the cesium ions is realized by an ordinary powder XRD pattern. Additionally, as a consequence of this work, it is synthesized a new type of struvite-like material.

Acknowledgment. This work was supported by FCT, project PTDC/CTM/108953/2008.

Supporting Information Available: X-ray crystallographic file in CIF format; tables of selected bond distances and bond valence calculations and powder X-ray patterns (PDF). This material is available free of charge via the Internet at http://pubs.acs.org.